

Transfer Learning between Motor Imagery Datasets using Deep Learning - Validation of Framework and Comparison of Datasets ^{*}

Pierre Guetschel^{1,2}[0000-0002-8933-7640] and
Michael Tangermann^{1,2}[0000-0001-6729-0290]

¹ Donders Institute for Brain, Cognition and Behaviour,
Radboud University, Nijmegen, Netherlands

² <first>.<last>@donders.ru.nl

Abstract. We present a simple deep learning-based framework commonly used in computer vision and demonstrate its effectiveness for cross-dataset transfer learning in mental imagery decoding tasks that are common in the field of Brain-Computer Interfaces (BCI). We investigate, on a large selection of 12 motor-imagery datasets, which ones are well suited for transfer, both as donors and as receivers.

Challenges. Deep learning models typically require long training times and are data-hungry, which impedes their use for BCI systems that have to minimize the recording time for (training) examples and are subject to constraints induced by experiments involving human subjects. A solution to both issues is transfer learning, but it comes with its own challenge, i.e., substantial data distribution shifts between datasets, subjects and even between subsequent sessions of the same subject.

Approach. For every pair of pre-training (donor) and test (receiver) dataset, we first train a model on the donor before training merely an additional new linear classification layer based on a few receiver trials. Performance of this transfer approach is then tested on other trials of the receiver dataset.

Significance. First, we lower the threshold to use transfer learning between motor imagery datasets: the overall framework is extremely simple and nevertheless obtains decent classification scores. Second, we demonstrate that deep learning models are a good option for motor imagery cross-dataset transfer both for the reasons outlined in the first point and because the framework presented is viable in online scenarios. Finally, analysing which datasets are best suited for transfer learning can be used as a reference for future researchers to determine which to use for pre-training or benchmarking.

Keywords: EEG · BCI · Motor Imagery · Deep Learning · Transfer Learning · Cross-Dataset

^{*} Supported by the Donders Center for Cognition (DCC).

1 Introduction

Electroencephalography (EEG) offers a non-invasive modality for capturing the electrical activity of the brain. Utilizing machine learning techniques, specific brain activities can be decoded in single trial. For instance, event-related potentials (ERPs) signify the brain’s response to the occurrence of an awaited and attended event [17]. Likewise, the sensorimotor cortices, being relatively large areas of the cortical surface, allow for the decoding of motor execution and motor imagery activities. The decoded brain activities can be mapped to computer commands. In so-called Brain-Computer Interfaces (BCIs) [4], the commands are used to drive applications that are directly controlled by the brain.

In a typical setting, each BCI session starts with an initial phase where the user is prompted to produce predefined outputs. This is typically called the *calibration phase*. The acquired data enables the supervised training of a decoding model. Only afterwards, the user can interact freely with the BCI application. This productive phase is typically called the *online mode*. However, calibration can be a tedious and uninteresting process for a user, and may require up to an hour of attention-demanding activities, even though the interesting phase we aim to start with as quickly as possible is the online phase.

Specifically for BCIs that make use of motor imagery tasks, the tedious calibration process prompts the consideration of Transfer Learning (TL) methods. TL leverages information from various sources, such as earlier sessions of the same user, of other users, or datasets obtained under slightly different experimental conditions, to reduce the need for calibration data samples collected during the ongoing session. In the most rudimentary approach to TL, a model is trained on a dataset we will call *donor*, and tested on another one we will call *receiver*. The necessity for TL becomes even more pronounced in the context of deep learning, given its inherent requirements for large training datasets and a substantial training time which would further delay the online phase [10]. However, TL presents its own challenges in the form of distributional shifts across different datasets, subjects, or even sessions. They can be attributed to factors like variations in experimental protocol, EEG recording systems, brain morphology, level of fatigue, medication intake, and more [11]. While TL has been widely studied in BCI, the focus has been mostly on cross-session transfer [30], cross-subject transfer [21,13], or both [14]. However, cross-dataset transfer learning has been a relatively underexplored domain. The recent BEETL competition has begun to fill this void by drawing attention to the challenges and opportunities cross-dataset transfer represents for BCI [26]. Notably, the top three winning methods in this competition were based on deep learning, thus indicating promising potential for such models. Furthermore, it was recently suggested to use cross-dataset transfer to evaluate the structure of cognitive tasks [1].

In this study, we extend a TL method already standard in the field of computer vision, the ImageNet linear evaluation protocol [5], to BCIs. Following our previous work which showcased its efficacy for cross-subject transfer [9], here we focus on its applicability for cross-dataset transfer. We experiment with one-

to-one transfer across twelve motor imagery datasets, leveraging the MOABB library [12] for both, dataset acquisition and normalized evaluation.

In this article, we will examine several pertinent questions: How challenging is actually TL between motor imagery datasets? Is deep learning genuinely a good option for TL in BCI? If so, what constitutes the minimal configuration necessary? Which datasets serve as the most effective donors? And which datasets are the best receivers? Our contributions can be summarized as follows:

1. We present a TL framework that can deal with a minimum of data from the receiver dataset and still reach good performance;
2. We lower the threshold to use TL between motor imagery datasets considering the extreme simplicity of this framework;
3. We provide evidence that deep learning models and our TL framework are apt choices for cross-dataset transfer, further substantiated by the viability of our framework for online scenarios;
4. We characterize the motor imagery datasets currently available in MOABB;
5. We present an analytical investigation into the suitability of these datasets for TL, serving as a valuable resource for future research in pre-training or benchmarking models.

Supplementary materials, including source code, pre-trained models, and comprehensive results, are available online³⁴.

2 Materials

2.1 Neural Network Architecture: EEGNet

We used EEGNet [15] as neural network architecture to conduct our experiments. It consists of an initial temporal convolutional layer that captures temporal correlations in EEG signals. This is followed by a depthwise spatial convolution layer that accounts for spatial correlations across electrodes. The network concludes with a separable convolution for dimensionality reduction before reaching the linear classification layer.

Our choice of EEGNet as the neural network architecture is motivated by three primary factors. First, its versatility is demonstrated through proficient performance across multiple BCI paradigms [15]. Second, its simplicity and computational efficiency make it particularly lightweight. Third, EEGNet has earned widespread community acceptance for EEG decoding, as evidenced by several studies [27,19,30,24,20,6].

2.2 Data: Motor Imagery

We conducted our experiments on EEG-based motor imagery (MI) datasets. They are constituted of EEG recordings capturing subjects as they either imagine or execute specific motor tasks. These motor tasks can range from imagined

³ Source code: https://gitlab.com/PierreGtch/motor_embedding_benchmark

⁴ Pre-trained models, and results: <https://huggingface.co/PierreGtch/EEGNetv4>

actions such as squeezing a fist to wiggling toes. In each dataset, multiple motor imagery tasks are represented and the classification problem is to determine which task was imagined/executed in each example, which typically consists of a few seconds of EEG recordings called a trial.

Table 1. Summary of Datasets Evaluated in the Study.

Dataset	Classes	No. classes	No. subjects	No. sessions	No. examples
AlexMI [2]	<i>f, r, rh.</i>	3	8	1	20
BNCI2014001 [25]	<i>f, lh, rh, t.</i>	4	9	2	72
BNCI2014004 [16]	<i>lh, rh.</i>	2	9	5	72
BNCI2015001 [7]	<i>f, rh.</i>	2	13	3 (subj. 8-11), 2 (others)	100
BNCI2015004 [22]	<i>f, n, rh, s, wa.</i>	5	9	2	39
Cho2017 [3]	<i>lh, rh.</i>	2	53	1	101
Lee2019_MI [16]	<i>lh, rh.</i>	2	55	2	200
Ofner2017 [18]	<i>r, ree, ref, rhc,</i> <i>rho, rp, rs.</i>	7	15	1	60
PhysionetMI [8]	<i>bh, f, lh, r, rh.</i>	5	109	1	23
Schirrmester2017 [23]	<i>f, lh, r, rh.</i>	4	14	1	241
Weibo2014 [28]	<i>bh, f, lh, lhrf,</i> <i>r, rh, rhlf.</i>	7	10	1	79
Zhou2016 [29]	<i>f, lh, rh.</i>	3	4	3	50

Description of Datasets In this study, we included all the Motor Imagery datasets available with the MOABB library [12]. However, three datasets were excluded due to technical limitations such as missing electrode names and impossibility of downloading the data. The complete list of datasets that were included along with their respective descriptions can be found in Table 1. The column "No. examples" designates for each dataset the number of examples/trials contained for each combination of subject, session and class. The imagined tasks which form the class label information in each dataset are described using the following abbreviations:

- *bh*: both hands
- *f*: both feet
- *lh*: left hand
- *lhrf*: left hand right foot
- *n*: navigation
- *r*: rest
- *ree*: right elbow extension
- *ref*: right elbow flexion
- *rh*: right hand
- *rhc*: right hand close
- *rhlf*: right hand left foot
- *rho*: right hand open
- *rp*: right hand pronation
- *rs*: right hand supination
- *s*: subtraction
- *t*: tongue
- *wa*: word association

It is noteworthy that the datasets included in this study employ diverse imagination strategies. For example, the Lee2019 dataset required subjects to imagine grasping with the appropriate hand. In contrast, the Cho2017 dataset instructed subjects to imagine moving their fingers from the index to the little finger. The Schirrneister2017 dataset contains executed instead of imagined movements, where subjects engaged in sequential finger-tapping. Of particular note is the Ofner2017 dataset, which includes *single* instances of both executed and imagined movements, diverging from other datasets that sustain or repeat the imagination tasks over several seconds. Some authors did not report the explicit instructions they gave on the imagination strategies and might have left it to the discretion of the subjects.

Pre-processing The pre-processing protocol we used for all the datasets involved setting the trial windows to 0 to 3 seconds post-cue. We strongly limited the EEG channels used to channels C3, C4, and Cz, which are placed over the sensorimotor cortices. The data was resampled at a frequency of 128Hz, aligning with EEGNet’s default setting. A bandpass filter with the range 0.5 to 40 Hz was applied to the data.

3 Method

In the current study, we employ the transfer learning framework previously proposed in our work [9]. However, a salient distinction is that, unlike the prior study which focused solely on cross-subject transfer, the present study extends this to cross-dataset transfer. A schematic representation of this methodology is encapsulated in Figure 1. This transfer framework has two phases: a pre-training phase using the donor dataset and a fine-tuning phase using the receiver dataset.

Pre-training Phase During the pre-training phase, a neural network architecture is trained from scratch on a set of source datasets, or donors. The aim is to categorize the motor task being imagined in each example/trial. To maintain a simple framework, the hyperparameters chosen are consistent with those recommended by the EEGNet authors for cross-subject training [15]. Upon completion of this phase, the network’s classification head is discarded, and the rest of the architecture is frozen, i.e., the remaining parameters will stay unchanged in the following phase.

Fine-tuning Phase In the subsequent fine-tuning phase, the pre-trained network is utilized as a feature extractor, wherein its parameters are frozen. A following linear classification layer is then trained from scratch to categorize the embeddings produced by the feature extractor. This classification layer is trained and tested using examples from the same session, i.e. the receiver dataset, adopting a within-session cross-validation (CV) approach through multiple random

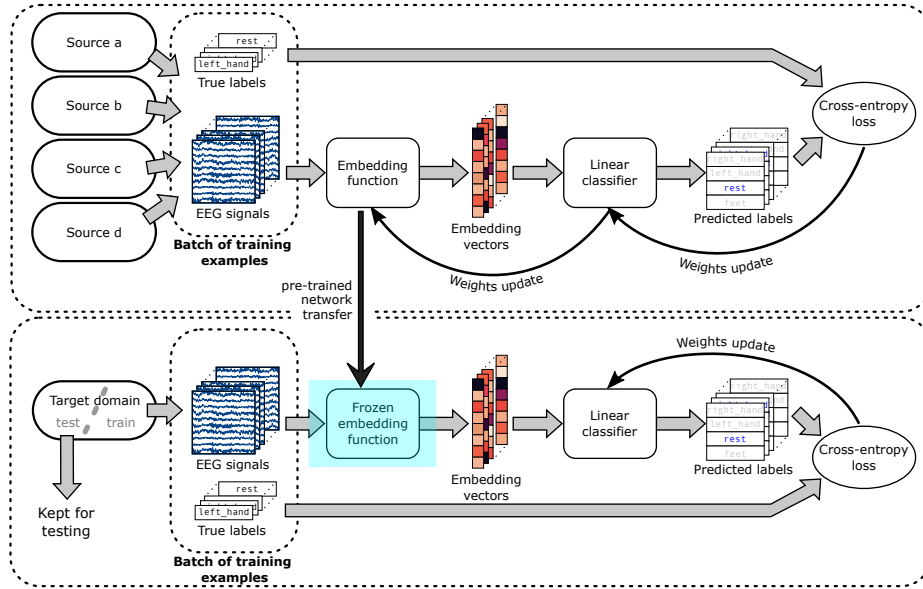


Fig. 1. Schematic representation of the transfer learning framework we introduced in [9] and have now extended to cross-dataset transfer. The upper block describes the pre-training phase. The lower block describes the fine-tuning phase.

shuffles of the examples. Importantly, during the fine-tuning phase, only the linear classification layer is subject to training, while the rest of the architecture remains static. The examples used to train the linear classification layer will be called *calibration examples*. The dataset employed for this fine-tuning is interchangeably termed as the *receiver dataset*, *test dataset* or *calibration dataset*, given that both fine-tuning and testing are executed within the same session of a single dataset, even though using separate examples.

4 Results

4.1 Experimental Settings

Pre-training Phase In this phase, a distinct EEGNet architecture was trained for each dataset, utilizing the entire dataset and all available classes therein. Consequently, a total of 12 pre-trained neural network architectures were generated.

Fine-tuning Phase During fine-tuning, we systematically examined varying numbers of calibration examples—specifically 1, 2, 4, 8, 16, 32 (where applicable), and 64 (where applicable) per class—across each session for every subject in the test datasets. Three distinct analyses were conducted: left hand vs. right hand (*lh-rh*), right hand vs. feet (*rh-f*), and an all-classes classification. The

classes specified for each analysis, are the only ones from the receiver used during the fine-tuning phase. The ROC-AUC (area under the receiver operating characteristic curve) metric was adopted for *lh-rh* and *rh-f* classification scores, while accuracy metrics were used for the all-classes scenario. The first two binary classification analyses allow for a fair comparison between datasets. Whereas the classification with all classes is a fallback case in which the chance level varies with the number of classes. We specifically focussed our analysis on the *lh-rh* and *rh-f* class pairs, as they are the most ubiquitously represented across the various datasets. The number of folds for within-session CV is set to 16. While this may appear excessive, it is crucial to mitigate the significant impact that the selection of just one or two calibration examples can have on the classification performance metrics.

4.2 Interpretation of Results

Data Volume and Analysis The three analyses culminated in an extensive set of 871,488 scores, derived from the different CV folds, number of calibration examples, sessions, subjects, test datasets, and pre-trained models.

Tabulated Scores For ease of interpretation, scores were averaged across CV folds, sessions, and subjects. This resulted in three summary tables corresponding to each of the three analytical scenarios. Each table contains an average score for every unique combination of pre-training dataset, test dataset, and number of calibration examples. Due to editorial limitations, the main text includes only black-and-white tables restricted to the case with 16 calibration examples per class. 16 calibration examples per class represents the maximum number that allows for the inclusion of all test datasets in the analysis. However, the complete color-coded tables are available in the supplementary materials, the location of which was indicated in the introductory section 1. Results of the *rh-f* analysis with 16 calibration examples per class are in Table 2(a), those related to the *lh-rh* one are in Table 2(b), and those covering the all-classes one can be located in Table 2(c).

Graphical Representations Line plots showing test scores with respect to the number of calibration example per class were generated from tabulated results, averaged either across test datasets in Figure 2 or pre-training datasets in Figure 3. Notably, in the averaged line plots, the datasets, even with disparate subject counts, hold equal weight.

Specific Observations and Cautions The crenellated blue line on the right-hand y-axis of Figure 2, denotes the number of test datasets included in each average. Its fluctuation is attributed to the variable number of examples across test datasets which does not allow to include all the datasets when using 32 or 64 calibration examples. Consequently, the average curves' progressions should be

interpreted only when the dataset count remains constant. When the number of test datasets included in the average decreases, an increase or decrease in score can respectively be explained by the disappearance of a "difficult" or an "easy" dataset.

In contrast, when averaging across pre-training datasets, i.e. Figure 3, the termination of each test dataset line is evident, and in some instances, extrapolation can provide insights into future trends.

It should be noted that scores obtained from the all-classes analyses require cautious interpretation due to varying class numbers across test datasets, which consequently alter the chance levels of accuracy scores.

Table 2. Scores using 16 Calibration Examples per Class

	(a) <i>f-rh</i> - AUC Score								(b) <i>lh-rh</i> - AUC Score								(c) All - Accuracy Sc.							
Test dataset	AlexMI	BNCI2014001	BNCI2015001	BNCI2015004	PhysionetMI(I)	Schirrneister2017	Weibo2014	Zhou2016	BNCI2014001	BNCI2014004	Cho2017	Lee2019_MI	PhysionetMI(I)	Schirrneister2017	Weibo2014	Zhou2016	AlexMI	BNCI2014001	BNCI2015004	Ofer2017(I)	PhysionetMI(I)	Schirrneister2017	Weibo2014	Zhou2016
Pretraining dataset																								
AlexMI	63	66	57	51	60	81	54	60	61	64	62	56	65	64	51	56	43	37	23	17	34	46	23	41
BNCI2014001	73	85	71	53	67	92	72	89	81	75	66	69	72	65	64	83	49	56	25	18	38	58	32	68
BNCI2014004	72	70	67	55	63	86	71	85	71	87	64	70	66	68	69	86	45	41	23	15	31	53	29	68
BNCI2015001	70	77	79	53	67	90	80	89	72	73	64	66	66	63	64	78	48	47	23	18	34	53	30	63
BNCI2015004	52	65	57	52	56	76	51	60	58	65	62	55	63	64	50	57	34	34	23	16	32	43	22	41
Cho2017	56	61	57	49	61	70	51	65	66	72	74	60	70	62	52	65	36	34	21	16	31	37	20	46
Lee2019_MI	74	75	71	51	70	88	78	90	79	82	68	77	75	72	77	91	48	47	23	17	33	53	32	74
Ofer2017(I)	50	50	50	50	50	50	50	50	50	50	55	50	50	50	50	50	33	24	20	17	12	25	14	33
PhysionetMI(I,E)	78	82	73	56	71	92	77	88	72	70	65	68	74	65	64	80	56	51	25	17	43	60	36	67
Schirrneister2017	74	80	75	51	67	96	77	91	74	73	64	70	68	69	66	84	54	50	23	17	35	66	33	69
Weibo2014	71	78	69	54	67	89	72	83	68	69	65	63	71	64	57	66	46	46	23	18	38	54	31	55
Zhou2016	71	75	74	53	67	88	78	95	75	78	66	72	69	70	70	93	49	46	24	17	34	54	32	80

4.3 Datasets as Donors

Referring to Figure 2, which illustrates averages across test datasets, the model pre-trained on Ofer2017 consistently performed at chance level. This outcome aligns with the dataset's distinct characteristics, as elaborated in section 2.2. Across the three classification scenarios, models pre-trained on the donor datasets AlexMI, BNCI2015004, or on Cho2017 underperformed. For the *rh-f* classification task, no single model emerged as a clear frontrunner. However, models pre-trained on the donor datasets PhysionetMI, Schirrneister2017, BNCI2014001, Zhou2016, Lee2019, or BNCI2015001 constituted the leading group. In the *lh-rh* classification task, the model pre-trained on Lee2019 demonstrated a distinct advantage.

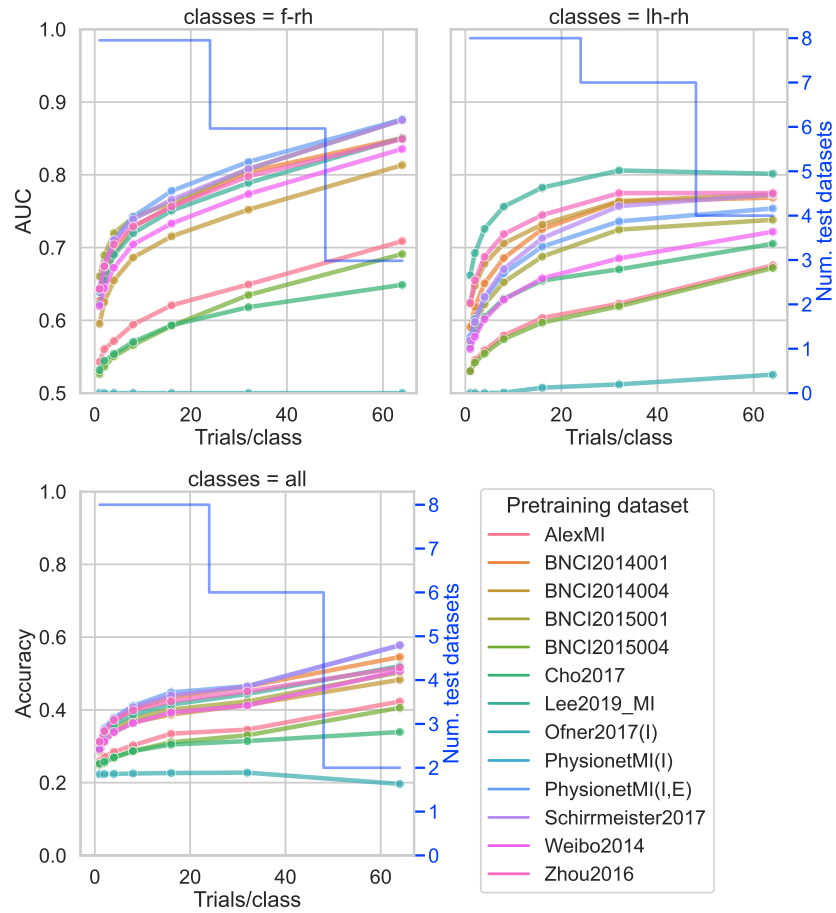


Fig. 2. Average Scores across Test Datasets

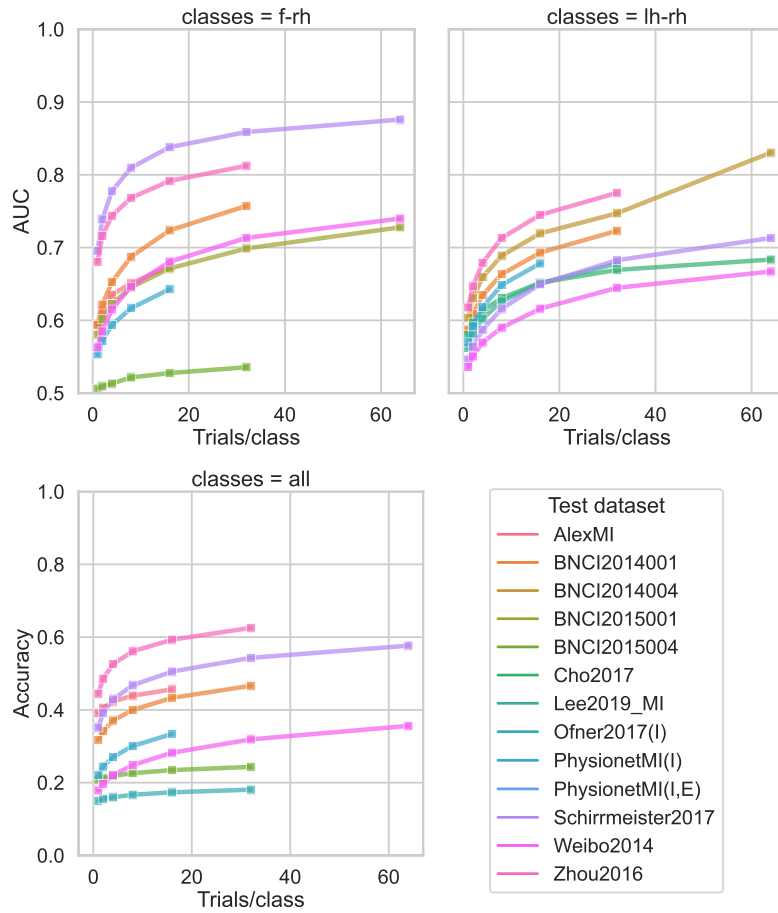


Fig. 3. Average Scores across Pre-training Datasets

Scores incorporating all classes from the test datasets are delicate to interpret and are presented primarily for informational purposes.

4.4 Datasets as Receivers

Turning our attention to Figure 3, which displays averages across pre-training datasets, we observe the following:

f-rh analysis Schirrmeister2017 emerges as the most straightforward dataset to classify, followed by Zhou2016 and then BNCI2014001. Conversely, BNCI2015004 and PhysionetMI proved most challenging, with performance nearing chance levels for BNCI2015004.

rh-lh analysis Zhou2016 demonstrated greater ease of classification relative to other datasets, succeeded by BNCI2014004 and then BNCI2014001. The most challenging datasets for this task are Weibo2014, followed by Lee2019, Cho2017, and Schirrmeister2017.

All-classes analysis In this context, Zhou2016 and Schirrmeister2017 were the easiest datasets to classify. Notably, none of the pre-trained models supplied features conducive to classifying Ofner2017 and BNCI2015004, with performance for both hovering at chance level.

5 Discussion

5.1 On the Datasets Evaluated

Lee2019 emerges as a highly favorable option for pre-training models for a simple *lh-rh* paradigm. Remarkably, even our rudimentary model attains competent classification scores across diverse datasets with very few calibration examples. This is likely attributable to its substantial number of subjects and examples.

PhysionetMI can serve as an interesting benchmark. Its low ranking when averaged across pre-training datasets implies inherent challenges. Moreover, its large number of subjects (109) implies also a large diversity. Furthermore, its positive performance during pre-training suggests that the task encapsulated is not overly divergent from those in other datasets. For the same reasons, Cho2017 and Lee2019 can also both serve as challenging benchmarks but they are limited to the *lh-rh* paradigm owing to class restrictions. Conversely, Zhou2016 and BNCI2014001 appear to be relatively uncomplicated benchmarks, consistently ranking among the top-performing receivers.

Schirrmeister2017 distinguishes itself as both a good donor and receiver. Its performance as a receiver can likely be attributed to the fact that it contains executed motor tasks, which are generally more straightforward to classify than imagined ones. Its strong performance as a donor is probably due to the higher number of examples available per subject, setting it apart from other datasets in the study.

The consistent chance-level performance observed with the Ofner2017 dataset, both as a donor and receiver, aligns with expectations given its marked divergence from the dataset pool, as outlined in section 2.2. The signal modality reported by its authors more closely resembles an event-related potential (ERP) than the oscillatory desynchronization or synchronization features typically observed for (motor) imagery tasks.

On a final note, pre-training models using a single dataset only probably is sub-optimal, and we opted for this simple approach solely for the purpose of our donor / receiver analysis. Instead, leveraging a diverse collection of donor datasets could enhance model generalizability.

5.2 On the Transfer Learning Framework

The transfer learning scheme presented is already widely utilized in the computer vision domain [5]. We posit that its broader adoption within the BCI community would be beneficial for multiple reasons:

First, the proposed framework has deliberately low complexity, eschewing ambiguous choices as we did not converge to it through prior testing. We adopted EEGNet, a common architecture in the BCI landscape, and adhered strictly to author-recommended parameters. Additionally, our reliance on merely three EEG channels reflects the simplicity of the chosen approach.

Our framework successfully accomplishes motor-imagery cross-dataset transfer learning, despite it being known as a difficult problem. Our results, which are proximal to state-of-the-art algorithms evaluated⁵ despite using fewer session examples, attest to this. Naturally, there is a maximal dissimilarity between datasets after which the transfer becomes impossible. We found that limit with the Ofner2017 dataset.

The efficiency of our framework is emphasized by our expansive analysis involving 871,488 classifiers. Such a broad analysis would be computationally prohibitive without a rapid fine-tuning mechanism.

Following the same idea, the swiftness of our fine-tuning strategy makes it suitable for online scenarios, without necessitating prolonged waiting periods for subject-specific model training as only a linear classification layer needs to be trained, which can be done in a few seconds on any recent CPU.

The modular nature of the two-phased framework allows for independent enhancements, facilitating the seamless incorporation of emerging deep learning techniques in both the embedding and fine-tuning stages. Because of the current simplicity of all its steps, we can expect large performance enhancement from improvements at any level. A first straightforward improvement would be to include additional EEG channels.

Finally, our framework demonstrates a pathway for utilizing deep learning models for BCI decoding. This approach effectively mitigates two challenges

⁵ For a comprehensive understanding of the state-of-the-art, the reader is advised to consult the MOABB benchmark [12], in conjunction with its forthcoming 2023 update.

inherent to deep learning techniques: the extensive requirement for data and lengthy training durations.

References

1. Aristimunha, B., de Camargo, R.Y., Pinaya, W.H.L., Chevallier, S., Gramfort, A., Rommel, C.: Evaluating the structure of cognitive tasks with transfer learning (Jul 2023). <https://doi.org/10.48550/arXiv.2308.02408>
2. Barachant, A.: Commande robuste d'un effecteur par une interface cerveau machine EEG asynchrone. Ph.D. thesis, Université de Grenoble (Mar 2012)
3. Cho, H., Ahn, M., Ahn, S., Kwon, M., Jun, S.C.: EEG datasets for motor imagery brain-computer interface. *GigaScience* **6**(7) (Jul 2017). <https://doi.org/10.1093/gigascience/gix034>
4. Clerc, M., Bougrain, L., Lotte, F.: *Brain-Computer Interfaces 2*. Wiley-ISTE (Jul 2016)
5. Deng, J., Dong, W., Socher, R., Li, L.J., Li, K., Fei-Fei, L.: ImageNet: A large-scale hierarchical image database. In: 2009 IEEE Conference on Computer Vision and Pattern Recognition. pp. 248–255 (Jun 2009). <https://doi.org/10.1109/CVPR.2009.5206848>
6. Deng, X., Zhang, B., Yu, N., Liu, K., Sun, K.: Advanced TSGL-EEGNet for Motor Imagery EEG-Based Brain-Computer Interfaces. *IEEE Access* **9**, 25118–25130 (2021). <https://doi.org/10.1109/ACCESS.2021.3056088>
7. Faller, J., Vidaurre, C., Solis-Escalante, T., Neuper, C., Scherer, R.: Autocalibration and Recurrent Adaptation: Towards a Plug and Play Online ERD-BCI. *IEEE Transactions on Neural Systems and Rehabilitation Engineering* **20**(3), 313–319 (May 2012). <https://doi.org/10.1109/TNSRE.2012.2189584>
8. Goldberger, A.L., Amaral, L.A., Glass, L., Hausdorff, J.M., Ivanov, P.C., Mark, R.G., Mietus, J.E., Moody, G.B., Peng, C.K., Stanley, H.E.: PhysioBank, PhysioToolkit, and PhysioNet: Components of a new research resource for complex physiologic signals. *circulation* **101**(23), e215–e220 (2000). <https://doi.org/10.1161/01.CIR.101.23.e215>
9. Guetschel, P., Papadopoulou, T., Tangermann, M.: Embedding neurophysiological signals. In: 2022 IEEE International Conference on Metrology for eXtended Reality, Artificial Intelligence, and Neural Engineering (MetroXRaine). pp. 169–174. IEEE, Rome (Oct 2022). <https://doi.org/10.1109/metroxraine54828.2022.9967496>
10. Ian Goodfellow, Yoshua Bengio, Aaron Courville: *Deep Learning*. MIT Press (2016)
11. Jayaram, V., Alamgir, M., Altun, Y., Scholkopf, B., Grosse-Wentrup, M.: Transfer learning in brain-computer interfaces. *IEEE Computational Intelligence Magazine* **11**(1), 20–31 (2016). <https://doi.org/10.1109/MCI.2015.2501545>
12. Jayaram, V., Barachant, A.: MOABB: Trustworthy algorithm benchmarking for BCIs. *Journal of Neural Engineering* **15**(6), 066011 (Dec 2018). <https://doi.org/10.1088/1741-2552/aadea0>
13. Jeon, E., Ko, W., Yoon, J.S., Suk, H.I.: Mutual Information-Driven Subject-Invariant and Class-Relevant Deep Representation Learning in BCI. *IEEE Transactions on Neural Networks and Learning Systems* pp. 1–11 (2021). <https://doi.org/10.1109/TNNLS.2021.3100583>
14. Kobler, R., Hirayama, J.i., Zhao, Q., Kawanabe, M.: SPD domain-specific batch normalization to crack interpretable unsupervised domain adaptation in EEG. In: *Advances in Neural Information Processing Systems*. vol. 35, pp. 6219–6235 (Dec 2022). <https://doi.org/10.48550/arXiv.2206.01323>

15. Lawhern, V.J., Solon, A.J., Waytowich, N.R., Gordon, S.M., Hung, C.P., Lance, B.J.: EEGNet: A Compact Convolutional Network for EEG-based Brain-Computer Interfaces. *Journal of Neural Engineering* **15**(5), 056013 (Oct 2018). <https://doi.org/10.1088/1741-2552/aace8c>
16. Leeb, R., Lee, F., Keinrath, C., Scherer, R., Bischof, H., Pfurtscheller, G.: Brain-Computer Communication: Motivation, Aim, and Impact of Exploring a Virtual Apartment. *IEEE Transactions on Neural Systems and Rehabilitation Engineering* **15**(4), 473–482 (Dec 2007). <https://doi.org/10.1109/TNSRE.2007.906956>
17. Luck, S.J.: *An Introduction to the Event-Related Potential Technique*, Second Edition. MIT Press (Jun 2014)
18. Ofner, P., Schwarz, A., Pereira, J., Müller-Putz, G.R.: Upper limb movements can be decoded from the time-domain of low-frequency EEG. *PLOS ONE* **12**(8), e0182578 (Aug 2017). <https://doi.org/10.1371/journal.pone.0182578>
19. Raza, H., Chowdhury, A., Bhattacharyya, S., Samothrakis, S.: Single-Trial EEG Classification with EEGNet and Neural Structured Learning for Improving BCI Performance. In: 2020 International Joint Conference on Neural Networks (IJCNN). pp. 1–8 (Jul 2020). <https://doi.org/10.1109/IJCNN48605.2020.9207100>
20. Riyad, M., Khalil, M., Adib, A.: Incep-EEGNet: A ConvNet for Motor Imagery Decoding. In: El Moataz, A., Mammass, D., Mansouri, A., Nouboud, F. (eds.) *Image and Signal Processing*. pp. 103–111. *Lecture Notes in Computer Science*, Springer International Publishing, Cham (2020). https://doi.org/10.1007/978-3-030-51935-3_11
21. Samek, W., Meinecke, F.C., Müller, K.R.: Transferring Subspaces Between Subjects in Brain-Computer Interfacing. *IEEE Transactions on Biomedical Engineering* **60**(8), 2289–2298 (Aug 2013). <https://doi.org/10.1109/TBME.2013.2253608>
22. Scherer, R., Faller, J., Friedrich, E.V.C., Opisso, E., Costa, U., Kübler, A., Müller-Putz, G.R.: Individually Adapted Imagery Improves Brain-Computer Interface Performance in End-Users with Disability. *PLOS ONE* **10**(5), e0123727 (May 2015). <https://doi.org/10.1371/journal.pone.0123727>
23. Schirrmester, R.T., Springenberg, J.T., Fiederer, L.D.J., Glasstetter, M., Eggenesperger, K., Tangermann, M., Hutter, F., Burgard, W., Ball, T.: Deep learning with convolutional neural networks for EEG decoding and visualization. *Human Brain Mapping* **38**(11), 5391–5420 (2017). <https://doi.org/10.1002/hbm.23730>
24. Schneider, T., Wang, X., Hersche, M., Cavigelli, L., Benini, L.: Q-EEGNet: An Energy-Efficient 8-bit Quantized Parallel EEGNet Implementation for Edge Motor-Imagery Brain-Machine Interfaces. In: 2020 IEEE International Conference on Smart Computing (SMARTCOMP). pp. 284–289 (Sep 2020). <https://doi.org/10.1109/SMARTCOMP50058.2020.00065>
25. Tangermann, M., Müller, K.R., Aertsen, A., Birbaumer, N., Braun, C., Brunner, C., Leeb, R., Mehring, C., Miller, K., Mueller-Putz, G., Nolte, G., Pfurtscheller, G., Preissl, H., Schalk, G., Schlögl, A., Vidaurre, C., Waldert, S., Blankertz, B.: Review of the BCI Competition IV. *Frontiers in Neuroscience* **6** (2012). <https://doi.org/10.3389/fnins.2012.00055>
26. Wei, X., Faisal, A.A., Grosse-Wentrup, M., Gramfort, A., Chevallier, S., Jayaram, V., Jeunet, C., Bakas, S., Ludwig, S., Barmpas, K., Bahri, M., Panagakis, Y., Laskaris, N., Adamos, D.A., Zafeiriou, S., Duong, W.C., Gordon, S.M., Lawhern, V.J., Śliwowski, M., Rouanne, V., Tempczyk, P.: 2021 BEETL Competition: Advancing Transfer Learning for Subject Independence and Heterogenous EEG Data Sets. In: *Proceedings of the NeurIPS 2021 Competitions and Demonstrations Track*. pp. 205–219. PMLR (Jul 2022)

27. Xu, F., Miao, Y., Sun, Y., Guo, D., Xu, J., Wang, Y., Li, J., Li, H., Dong, G., Rong, F., Leng, J., Zhang, Y.: A transfer learning framework based on motor imagery rehabilitation for stroke. *Scientific Reports* **11**(1), 19783 (Oct 2021). <https://doi.org/10.1038/s41598-021-99114-1>
28. Yi, W., Qiu, S., Wang, K., Qi, H., Zhang, L., Zhou, P., He, F., Ming, D.: Evaluation of EEG Oscillatory Patterns and Cognitive Process during Simple and Compound Limb Motor Imagery. *PLoS ONE* **9**(12), e114853 (Dec 2014). <https://doi.org/10.1371/journal.pone.0114853>
29. Zhou, B., Wu, X., Lv, Z., Zhang, L., Guo, X.: A Fully Automated Trial Selection Method for Optimization of Motor Imagery Based Brain-Computer Interface. *PLOS ONE* **11**(9), e0162657 (Sep 2016). <https://doi.org/10.1371/journal.pone.0162657>
30. Zhu, Y., Li, Y., Lu, J., Li, P.: EEGNet With Ensemble Learning to Improve the Cross-Session Classification of SSVEP Based BCI From Ear-EEG. *IEEE Access* **9**, 15295–15303 (2021). <https://doi.org/10.1109/ACCESS.2021.3052656>